Matrix Biology Plus 24 (2024) 100162

Contents lists available at ScienceDirect

Matrix Biology Plus

journal homepage: www.sciencedirect.com/journal/matrix-biology-plus

Obesity-driven changes in breast tissue exhibit a pro-angiogenic extracellular matrix signature

Ellen E. Bamberg [a], Mark Maslanka [b], Kiran Vinod-Paul [a], Sharon Sams [c], Erica Pollack [d], Matthew Conklin [e,f], Peter Kabos [a,*], Kirk C. Hansen [b,*]

[a] Department of Medicine, Division of Medical Oncology, University of Colorado Anschutz Medical Campus, Aurora, CO, USA
[b] Department of Biochemistry and Molecular Genetics, University of Colorado Anschutz Medical Campus, Aurora, CO, USA
[c] Department of Pathology, University of Colorado Anschutz Medical Campus, Aurora, CO, USA
[d] Department of Radiology and Medical Imaging, University of Colorado Anschutz Medical Campus, Aurora, CO, USA
[e] Department of Cell and Regenerative Biology, School of Medicine and Public Health, Carbone Cancer Center (Tumor Microenvironment Program), University of Wisconsin, Madison, WI, USA
[f] Laboratory for Optical and Computations Instrumentation, Department of Biomedical Engineering, University of Wisconsin-Madison, Madison, WI, USA

ARTICLE INFO

Keywords:
Extracellular matrix
Tissue Proteomics
Peroxidasin
Galectin
PXDN
LGALS3
LGALS1
Breast
Obesity
Body Mass Index
Stromal cells
Fibroblasts
Adipocytes
Tumor Microenvironment

ABSTRACT

Obesity has reached epidemic proportions in the United States, emerging as a risk factor for the onset of breast cancer and a harbinger of unfavorable outcomes [1–3]. Despite limited understanding of the precise mechanisms, both obesity and breast cancer are associated with extracellular matrix (ECM) rewiring [4–6]. Utilizing total breast tissue proteomics, we analyzed normal-weight (18.5 to < 25 kg/m^2), overweight (25 to < 30 kg/m^2), and obese (≥30 kg/m^2) individuals to identify potential ECM modifying proteins for cancer development and acceleration. Obese individuals exhibited substantial ECM alterations, marked by increased basement membrane deposition, angiogenic signatures, and ECM-modifying proteins. Notably, the collagen IV crosslinking enzyme peroxidasin (PXDN) emerged as a potential mediator of the ECM changes in individuals with an elevated body mass index (BMI), strongly correlating with angiogenic and basement membrane signatures. Furthermore, glycan-binding proteins galectin-1 (LGALS1) and galectin-3 (LGALS3), which play crucial roles in matrix interactions and angiogenesis, also strongly correlate with ECM modifications. In breast cancer, elevated PXDN, LGALS1, and LGALS3 correlate with reduced relapse-free and distant-metastatic-free survival. These proteins were significantly associated with mesenchymal stromal cell markers, indicating adipocytes and fibroblasts may be the primary contributors of the obesity-related ECM changes. Our findings unveil a pro-angiogenic ECM signature in obese breast tissue, offering potential targets to inhibit breast cancer development and progression.

Introduction

Globally, the prevalence of obesity is escalating, with a projected 51 % of the world's population expected to be overweight or obese by 2035 [3]. In the United States, obesity affects a staggering 42.4 % of the adult population and has been identified as a significant risk factor for various cancers, including breast cancer [7]. In postmenopausal women, obesity confers up to a 1.33-fold increase in the likelihood of developing breast cancer [7]. Irrespective of subtype or menopausal status, obesity denotes aggressive disease development resulting in a worsened prognosis [2]. Obese breast cancer patients contend with higher tumor grades, poor treatment response, and a heightened propensity for locoregional and distal metastasis, which is increased by 46 % within 10 years post-diagnosis [2,4,7,8]. Furthermore, an increased BMI is associated with elevated mortality reflected by a significant decrease in both reoccurrence-free and overall survival [4,7,8].

The exact link between obesity and heightened breast cancer risk as well as worse outcomes is not fully understood. Current research widely points to hormonal, metabolic, inflammatory, and extracellular matrix (ECM) dysfunction as potential factors [4,7,9]. Excessive energy intake leads to rapid adipose tissue hypertrophy, causing an abnormal increase in growth factors, cytokines, adipokines, and estrogen [7,9]. These signals trigger the recruitment of macrophages, which form distinctive crown-like structures around hypertrophic adipocytes, and the

* Corresponding authors.
E-mail addresses: Peter.Kabos@cuanschutz.edu (P. Kabos), Kirk.Hansen@cuanschutz.edu (K.C. Hansen).

https://doi.org/10.1016/j.mbplus.2024.100162
Received 7 August 2024; Received in revised form 6 September 2024; Accepted 19 September 2024
Available online 22 September 2024

activation of fibroblasts [7,9]. This in turn initiates adipose tissue fibrosis and stromal stiffening, characterized by depositional and organizational changes to the ECM [4,9]. These ECM alterations can contribute to both breast cancer oncogenesis and disease progression [1,4,10].

Breast cancer development is accompanied by stromal fibrosis, resulting in ECM reorganization and stromal stiffening [5,9,11]. An aggressive tumor microenvironment (TME) is characterized by dysregulated ECM, such as elevated levels of collagen IV, V, and VI, fibronectin, and laminin [5,11]. Structurally collagen fiber orientation is altered to align perpendicular to the tumor border [11,12]. While stromal stiffening, through critical collagen cross-linking enzymes such as lysyl oxidase (LOX) and lysyl hydroxylase 2 (PLOD2), can cause mechanical signaling that promotes breast cancer dissemination [5,11]. These alterations play a pivotal role in driving oncogenesis, invasion, motility, and angiogenesis, collectively propelling cancer cells along the path of the metastatic cascade [5,11].

While mouse models of obesity have been used to assess protein level changes in mouse mammary fat pads [13,14], current clinical studies on obesity have largely focused on gene expression, often neglecting thorough protein-level analysis of human breast tissue [10]. Furthermore, in breast cancer studies utilizing BMI, proteomic methodologies have only been applied to plasma, limiting the relevance of links to components of ECM [15]. We hypothesized that obesity induces significant alterations in normal breast tissue's extracellular matrix (ECM) via enzymatic and depositional modifications. This study aimed to uncover specific targets that expedite the incidence of breast cancer within this vulnerable demographic. To address this, we employed samples acquired from the Komen tissue bank, primarily from post-menopausal women. Using a two-fraction ECM extraction method, designed to improve ECM peptide identification, we performed total tissue proteomics [16,17]. Here we identify a pro-angiogenic ECM signature underlying obese breast tissue samples, elucidating novel and targetable enzymes implicated in breast cancer outcomes. To our knowledge, this study is the sole collection of normal human breast tissue analyzed by BMI status and using a novel approach to ECM-focused tissue proteomics, addressing a significant gap in current breast cancer research.

Results

Normal breast samples across BMI were selected from the Komen Tissue Bank

This study was designed to explore the hypothesis that obesity alters the breast microenvironment in a manner that is conducive to oncogenic changes and is associated with poorer breast cancer outcomes. Breast tissue samples from the Komen Tissue Bank were obtained to accomplish this goal. Normal breast tissues were categorized by BMI at the time of tissue donation into three groups: normal-weight (18.5 to < 25 kg/m^2), overweight (25 to < 30 kg/m^2), and obese ($\geq$30 kg/m^2) (Table 1). The distribution of patients included nine samples from normal-weight individuals, six from overweight, and twelve from obese patients (Table 1 and Fig. 1a). Over half of the obese patients had a BMI in class I (30 to $<$ 35 kg/m^2), with the rest distributed between class II (35 to < 40 kg/m^2) and class III ($\geq$40 kg/m^2) (Fig. 1a and Supplementary Table 1). The samples encompass the body weight range commonly observed in peri- and post-menopausal individuals, where obesity is more prevalent due to changes in hormonal status [1,10,18]. Our selected participants, aged 45 to 75 years old, represented the typical age range for breast cancer diagnoses [12] (Table 1 and Supplementary Table 1). The majority of the chosen samples were from post-menopausal women, with only four individuals reported to be pre-menopausal (Supplementary Table 1). The cohort was predominately comprised of Caucasian women, with only two individuals identified as Black/African American and one as Asian/Chinese, which reflects the demographics of available samples within the Komen Tissue Bank (Supplementary Table 1).

Table 1
Summary of patient demographics.

	Total Number of Patients	Number of Breast Cancer Patients*	Average Age (Yrs)	Average BMI (kg/m^2)
Healthy	9	4	58	22.2
Overweight	6	5	52.2	28.4
Obese	12	8	56.8	35.2

* Refers to patients with a diagnosis of breast cancer before or following the donation of normal breast tissue.

Obesity rewires breast ECM towards a pro-angiogenic signature

To explore how BMI specifically contributes to changes in the ECM, we conducted total tissue proteomics on breast samples from normal-weight, overweight, and obese individuals. We assessed protein intensity differences between normal weight and overweight or obese samples (Fig. 1b). Obese patients exhibited a greater number of significantly elevated proteins compared to normal weight, whereas the difference between normal weight and overweight samples was minimal (Fig. 1b). Overweight individuals showed elevated proteins related to metabolism (HK3, UBE2G1, and ACOX1), protein homeostasis (DDX46 and EIF4G2), and ECM biology (CD248 and LGALS3) (Fig. 1b). The gene lists generated from these comparisons identified only 6 proteins consistently elevated in both overweight and obese samples (UBE2G1, CD248, DYNLL2, LGALS3, CD276, and PIN1) (Fig. 1b). Though few proteins overlapped in obese and overweight samples, shared protein families regulating protein homeostasis and metabolism were present (Fig. 1b), implying conserved pathway activation in these individuals.

Samples from obese individuals exhibited a notable increase in proteins associated with vesicle trafficking, protein homeostasis, metabolism, cell motility, and extracellular matrix (ECM) reorganization (Fig. 1b). Analysis of these samples revealed a variety of elevated ECM modifying proteins including cathepsins, annexins, galectins, and the collagen IV crosslinking enzyme peroxidasin (Fig. 1b, 1c, and Fig. S1a) [5,19–23]. The basement membrane components such as LAMA4, LAMB2, LAMC1, and COL15A1 were also elevated in the high BMI samples (Fig. 1b and Fig. S1a) [21,24]. Similarly, these proteins and other angiogenic and basement membrane regulators including F13A1, MFAP5, and NID2, a PXDN binding partner, positively correlated with increasing BMI (Fig. S1b) [25]. These compositional and ECM-modifying proteins have all been implicated in angiogenic processes and basement membrane formation [19–21,23,24].

In contrast to overweight or obese individuals, normal-weight individuals exhibited fewer significantly elevated proteins (Fig. 1b). The identified proteins were primarily linked to critical cell processes such as calcium homeostasis (CAMK2G) and cell adhesion (CDH1, ITGB4) (Fig. 1b). Moreover, a select few extracellular matrix (ECM) proteins, particularly collagen XXI (COL21A1) and collagen IV (COL7A1), were significantly elevated in normal weight individuals (Fig. 1b and 1c). The diminished presence of collagen VII, a potent suppressor of both TGF-β and angiogenesis, starkly contrasts with the heightened expression of ECM proteins, capable of promoting angiogenesis, in obese patients [26,27]. This implies a substantial shift in ECM composition between low and high BMI breast tissue samples, suggesting potential disruptions in normal basement membrane and angiogenic processes. Notably, CD248, a top hit in overweight and obese individuals, serves as a widely recognized marker for mesenchymal stromal cells, including fibroblasts and adipocytes [28–30]. Other fibroblast markers such as S100A4, SERPINH1, and VIM were also positively correlated with and significantly elevated in high BMI samples (Fig. 1b, Fig. 1c, and Fig. S1d) [31–33]. While immune cell markers showed no significant increase in overweight samples, obese individuals exhibited a notable elevation in the leukocyte marker CD45 and monocyte marker CD14 (Fig. 1b).

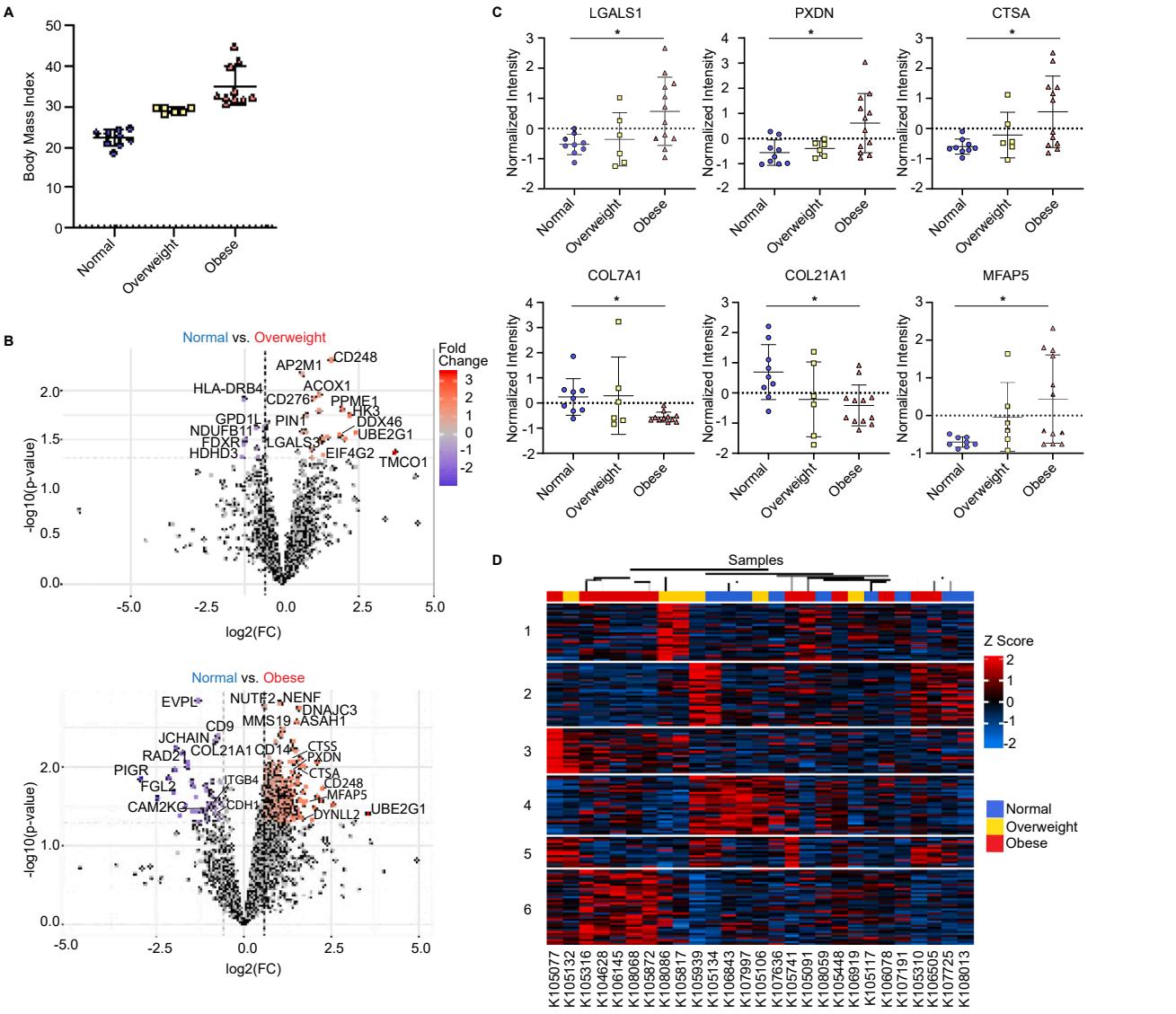

Fig. 1. Modulation of the breast ECM in obese individuals is reflective of pro-angiogenic signaling. **(A)** The distribution of BMI across patients was sorted into normal weight (BMI of 18.5 to < 25 kg/m^2), overweight (BMI of 25 to < 30 kg/m^2), and obese (BMI of ≥ 30 kg/m^2) populations. **(B)** Volcano plots compare significantly upregulated proteins, measured by normalized peak intensities in tissue proteomics, among obese (red), overweight (red), and normal-weight (blue) individuals. *Unpaired T-test* * $p \leq 0.05$; *Fold Change* ≥ 1.5. **(C)** Representative graphs of ECM proteins significantly elevated or decreased in patients grouped by BMI. *Kruskal-Wallis Test* * $p \leq 0.05$ **(D)** K-means clustering by total protein across the samples sub-divided by sample ID and BMI. (For interpretation of the references to colour in this figure legend, the reader is referred to the web version of this article.)

Absence of typical markers for T-cells, B-cells, NK cells, and dendritic cells in obese individuals suggests that fibroblasts, adipocytes, and macrophages play a primary role in the observed phenotypic differences in ECM composition.

We then performed hierarchical clustering of proteins across the samples to identify distinct patterns of proteins associated with BMI (Fig. 1d and S1c). High BMI predominantly correlated with clusters 1, 3, and 6 (Fig. 1d) No clear pattern emerged based on prior or subsequent breast related diagnosis (Fig. 1d). Pathway analysis indicated that clusters 1 and 6 were characterized by metabolism, angiogenesis, matrix organization, and immune signaling pathways, reinforcing their BMI-driven nature (Fig. 1d and S2). Cluster 3 exhibited similar pathway activation, but was primarily associated with protein homeostasis, aligning with our earlier analysis (Fig. 1d and S2). Cluster 2 exhibited pathways tied to RTK signaling, immune complement signaling, and matrix organization (Fig. 1d and S2).

We examined the distribution of ECM proteins across the clusters identified in our total proteomics data. Cluster 2 featured proteins traditionally linked to breast cancer progression, such as COLXII, COLVI, and MMP2 (Fig. 1d) [11,34]. In contrast, Cluster 6 was primarily characterized by ECM-modifying proteins, including LOXL1, PLOD1, PLOD2, and PXDN, which are all involved in collagen crosslinking (Fig. 1d) [5,19,20]. Additionally, Cluster 3 and 6 exhibited ECM proteins strongly associated with angiogenesis including cathepsin, annexin, laminins, and galectin-1 (Fig. 1d) [21–24]. Collagens XV and XVIII, also present in cluster 6, are bone-marrow-associated multiplexin collagens that line blood vessels and contribute to adipocyte differentiation [6,35]. Fibroblast markers also fell within cluster 6, in contrast to the macrophage marker CD14 which was present in cluster 5 (Fig. 1d). Cluster 1 was predominantly defined by ECM compositional proteins, including various collagens and fibronectin (Fig. 1d). Notably, other ECM-modifying proteins, namely MMP9, LGALS3, and PLOD3, were present in this cluster and are commonly correlated with breast cancer outcomes (Fig. 1d). Similar clusters emerged when the ECM proteins were isolated. In the ECM-only analysis, cluster 4 corresponds to the obesity-driven clusters identified in the total proteomics (Fig. S1c).

In summary, proteomic analysis of primary breast samples showcases distinct protein profiles in obese individuals, indicating a pronounced impact of BMI on ECM dynamics, many of which are implicated in angiogenic processes.

ECM-modifying proteins involved in angiogenesis correlate with worse breast cancer outcomes

We investigated the correlation between our proteomic data and elevated BMI to identify key targets associated with BMI increase. Among the top 25 proteins positively correlated with elevated BMI were

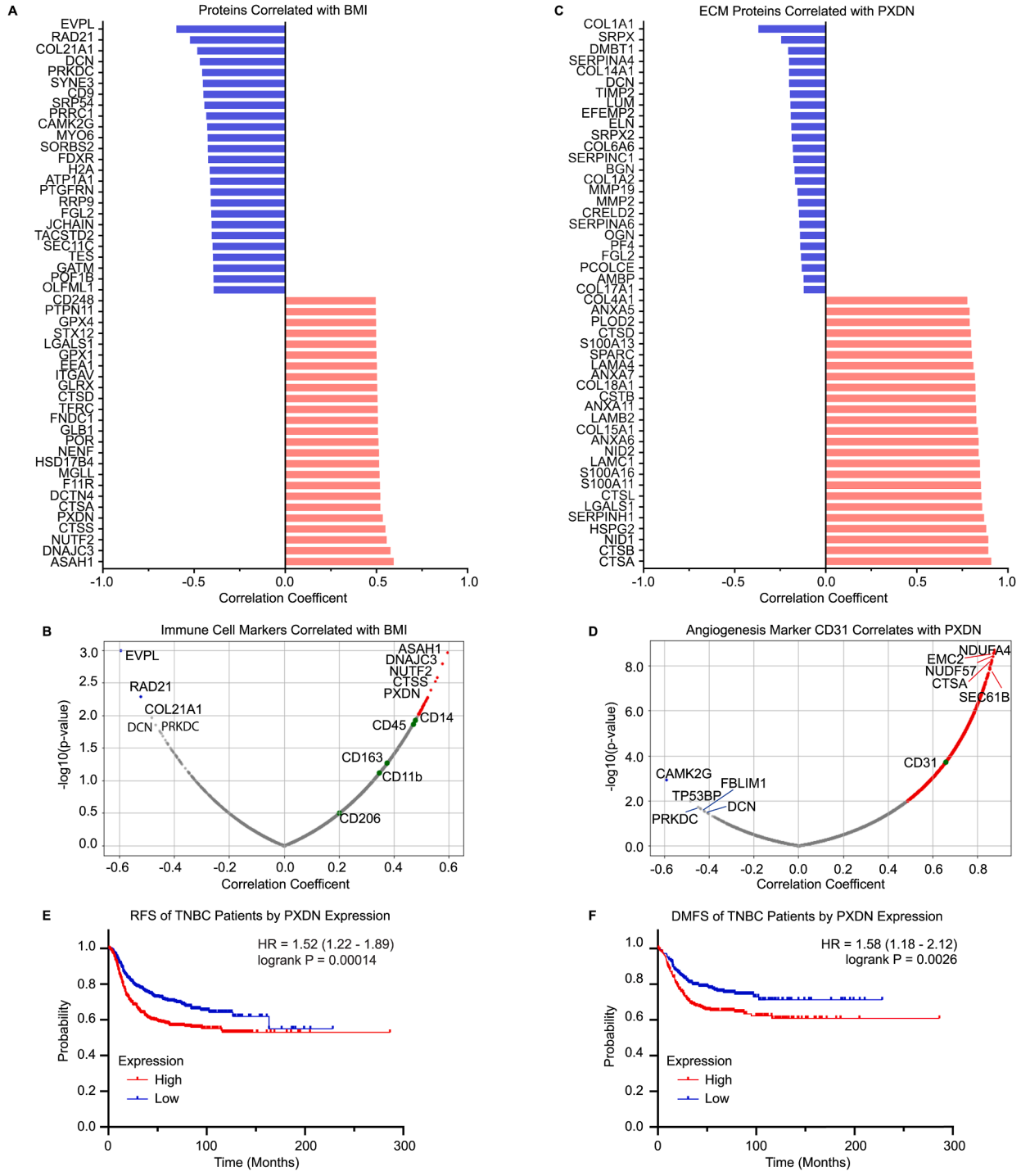

Fig. 2. High BMI correlates with pro-angiogenic ECM changes predictive of poor breast cancer outcomes. **(A)** Waterfall plot of the top 25 proteins correlated (red) or inversely correlated (blue) with BMI. **(B)** Graph plotting the correlation coefficient (r) against the significance (−log10(p-value)) indicates proteins significantly correlated (red) or inversely correlated (blue) with high BMI. The immune cell markers CD206, CD11b, CD163, CD14, and CD45 are highlighted in green. **(C)** Waterfall plot of the top 25 ECM proteins correlated (red) or inversely correlated (blue) with PXDN. **(D)** Graph plotting the correlation coefficient (r) against the significance (−log10(p-value)) indicates proteins significantly correlated (red) or inversely correlated (blue) with PXDN. The angiogenic marker CD31 was highlighted in green. *Pearson R correlation test* * $p \leq 0.05$, $r \geq 0.5$.* **(E)** RFS and **(F)** DMFS of TNBC patients by low or high PXDN expression. *Log-rank Test* ** $p \leq 0.01$, **** $p \leq 0.0001$, Hazard Ratio (HR) > 1.0.* (For interpretation of the references to colour in this figure legend, the reader is referred to the web version of this article.)

several ECM-modifying proteins, including cathepsins (CTSS, CTSA, and CTSD), peroxidasin (PXDN), and galectin-1 (LGALS1) (Fig. 2a and Fig. 2b). CD248, a mesenchymal stromal cell marker, was featured prominently among these top proteins, suggesting a significant role of fibroblasts and adipocytes in obesity (Fig. 2a). Additional markers such as VIM and SERPINH1 showed a positive yet insignificant correlation with BMI (Fig. S3a and S3b). We also examined the correlation between immune cell markers and BMI. A non-significant but positive correlation with obesity was observed for myeloid and macrophage markers CD14, CD163, CD11b, and CD206 (Fig. 2b). The only additional immune marker observed to correlate with BMI was the leukocyte common antigen CD45 (Fig. 2b). No other immune markers commonly used to identify lymphoid cells were present in the proteomic dataset.

We then aimed to identify ECM proteins specifically correlating with PXDN, the top-hit identified consistently throughout our proteomic analysis. PXDN exhibited a strong correlation with ECM proteins involved in angiogenesis and basement membrane formation (Fig. 2c). PXDN also showed a strong correlation with angiogenesis-regulating

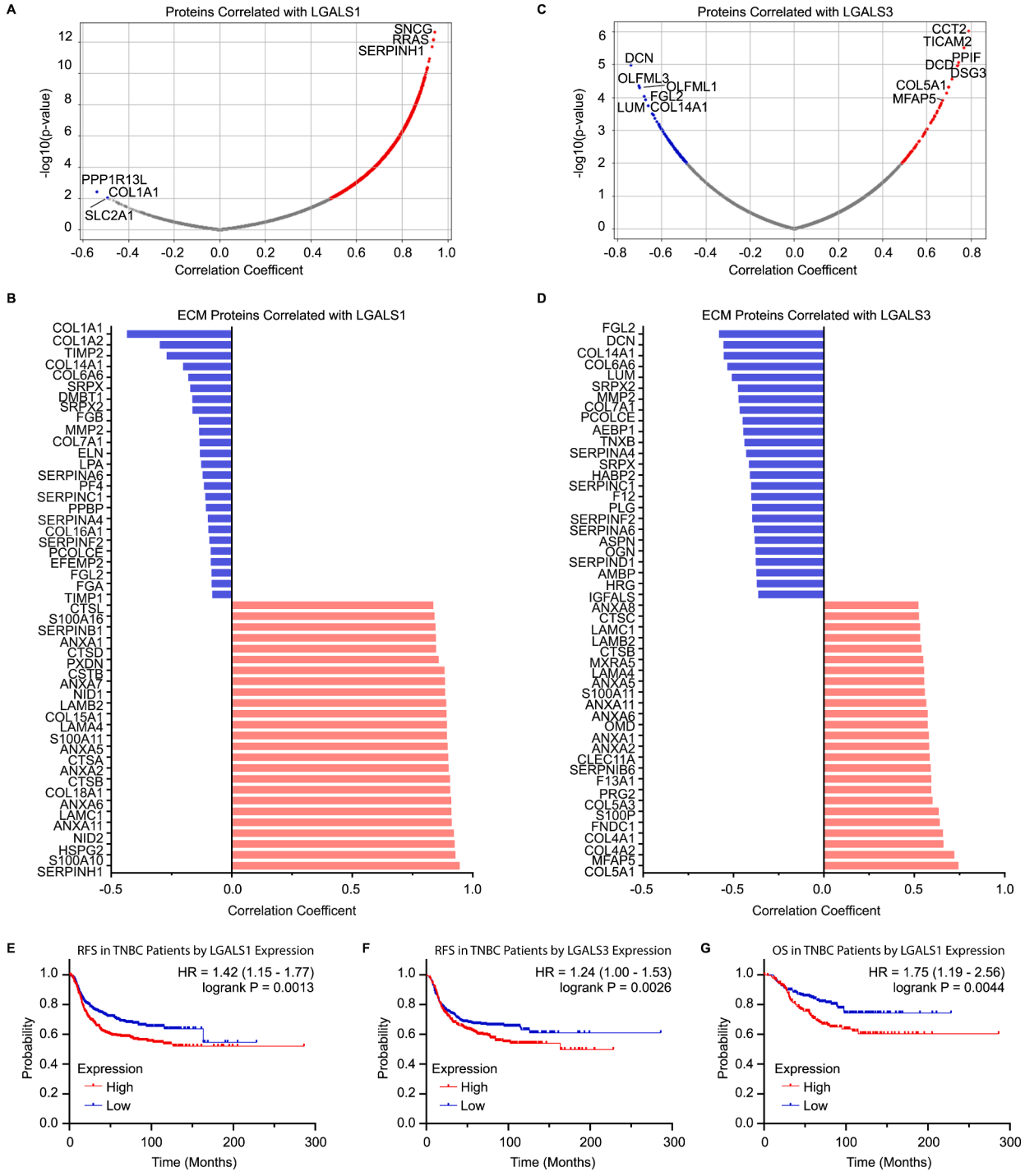

Fig. 3. LGALS1 and LGALS3 correlate with angiogenic ECM proteins and poor breast cancer outcomes. All proteins correlated with **(A)** LGALS1 and **(B)** LGALS3 were plotted to compare the correlation coefficient (r) against the significance (−log10(p-value)) for each protein. Waterfall plot of the top 25 ECM proteins correlated or inversely correlated with **(C)** LGALS1 and **(D)** LGALS3. *Pearson R correlation test* * $p \leq 0.05$, $r \geq 0.5$. RFS of TNBC patients based on **(E)** LGALS1 and **(F)** LGALS3 expression**. (G)** Overall survival (OS) of TNBC patients based on LGALS1 expression. *Log-rank Test* ** $p \leq 0.01$, **** $p \leq 0.0001$, *Hazard Ratio (HR)* > *1.0.*

ECM-modifying proteins, such as lysyl hydroxylase, cathepsins, nidogens, and annexins (Fig. 2c). As expected, structural laminins (LAMA4, LAMB2, and LAMC1) and collagen IV also exhibited a positive correlation with PXDN (Fig. 2c). PXDN significantly correlated with mesenchymal stromal cell markers (SERPINH1, VIM, CD248), and, albeit non-significantly, exhibited positive correlations with immune cell markers (CD14, CD11b, CD206) (Fig. S2c). This suggests that the mesenchymal stromal population plays a pivotal role as a major source of PXDN. In the broader context of total proteomics, PXDN was significantly and positively correlated with the endothelial cell marker CD31, commonly used for the identification of vasculature (Fig. 2d), further supporting an angiogenic phenotype.

Putting this finding in the context of breast cancer, we aimed to understand PXDN's role in breast cancer progression and prognosis. Elevated PXDN expression is associated with significantly reduced relapse-free survival (RFS) and distant metastasis-free survival (DMFS) in triple-negative breast cancer, widely acknowledged as one of the most aggressive subtypes (Fig. 2e and 2f). This association holds true for HER2-amplified breast cancer as well (Fig. S4a and 4b).

We analyzed two additional ECM-modifying proteins, LGALS1 and LGALS3, that were identified among the top 25 ECM proteins positively correlated to elevated BMI (Fig. S1a, S1b, and Fig. 3). LGALS1 showed a positive and negative correlation signature similar to PXDN, and it significantly correlated with fibroblast marker SERPINH1 (Fig. 3a and 3b). Notably, LGALS1 displayed a unique and significant inverse correlation with collagen VII, previously described as an angiogenic inhibitor (Fig. 3a and 3b)[27]. LGALS3 also positively correlated with angiogenic-promoting ECM and basement membrane proteins including collagen IV, collagen V, laminin, annexins, and cathepsins (Fig. 3c and 3d). It also distinctly correlated with MFAP5, which regulates endothelial cell motility (Fig. 3c and 3d) [36]. In the context of breast cancer, high expression of both LGALS1 and LGALS3 significantly correlated with reduced RFS (Fig. 3e and 3f). LGALS1 also correlated with reduced overall survival (OS) (Fig. 3g). These findings strongly link these

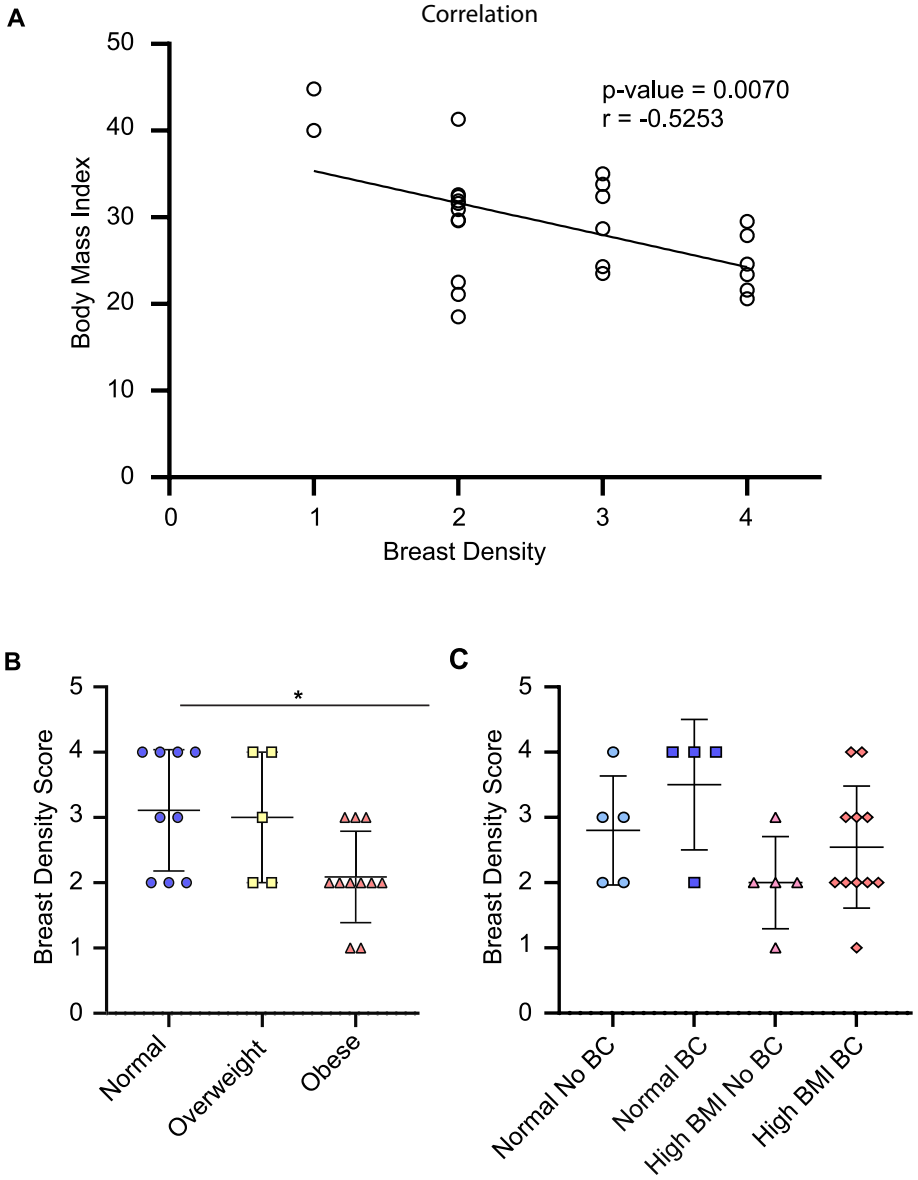

Fig. 4. Mammogram density declines in obese women. **(A)** The correlation of BMI to breast density score. *Simple Linear Regression.* **(B)** Breast density of women scored on a scale of least to most dense (1 to 4). Samples were sorted by body mass index (BMI) into normal weight, overweight, and obese populations. *Kruskal-Wallis Test* $* p \leq 0.05$. **(C)** Samples were categorized based on BMI into two groups: healthy and High BMI, overweight and obese individuals with a healthy BMI, and those with a high BMI, including overweight and obese individuals. Additionally, the samples were further divided based on breast cancer risk into two categories: individuals who never had breast cancer (No BC) or patients who previously had breast cancer, developed it, or reoccurred after tissue donation (BC).

proteins to obesity, emphasizing their potential to prime the obese tissue microenvironment for aggressive tumor growth and angiogenesis.

Breast density inversely correlates with BMI

Breast density is canonically a prognostic indicator of breast cancer risk, conferring up to a sixfold increase in the risk of developing breast cancer [37–39]. BMI is now considered a confounding variable in mammogram density assessment, necessitating its inclusion when categorizing breast tissue density [37,40]. To isolate the contribution of breast density to our data we measured breast density of the patient's mammograms using the Breast Imaging Reporting & Data System (BI-RADS) [42] (Fig. S4c). Other studies have shown an inverse relationship between breast density and BMI [18,41]. Indeed, we observed a significant decrease in the breast density of obese individuals, confirmed by the inverse correlation of BMI and breast density score (Fig. 4a and 4b). Despite this inverse relationship, both obesity and mammogram density have been described as independent risk factors for breast cancer development, with varying reports on their interconnection [18,37].

All samples were identified as normal breast tissue at the time of donation, however several of the included samples were from women who either had a prior diagnosis or later developed breast cancer. Among the 27 patients, mammogram data for 10 patients without a history of breast cancer, 4 in remission, 7 that developed breast cancer, and 4 that later experienced reoccurrence (Table 1, Supplementary Tables 1 and 2) were available. Although there was a modest trend of elevated breast density in patients who were in remission and those who later developed breast cancer, the difference was not statistically significant, possibly due to the small sample size (Fig. S5a). When grouping samples by BMI into healthy and overweight/obese categories and then subdividing by breast cancer diagnosis, individuals with a prior or subsequent breast cancer diagnosis exhibited a trend towards increased breast density (statistically not significant, Fig. 4c).

In patients grouped by breast cancer risk, proteomic analysis revealed that those with recurrences showed the highest differential protein expression, in contrast to individuals without breast cancer. Those who developed breast cancer post-tissue donation showed limited differential protein expression when compared to those without breast cancer (Fig. S5b and S5c). Volcano plots (Fig. S5b) showed minimal conserved proteins between individuals without breast cancer and those at risk, with the cytoskeletal marker cytokeratin-17 (KRT-17) being the sole conserved protein (Fig. S5b) [42]. When samples were clustered no clear trend dictated by breast cancer risk emerged (Fig. S5c). Few ECM proteins were significantly elevated in those with a prior or subsequent diagnosis of breast cancer compared to those without, with the signal mainly originating from recurrent patients (Fig. S5b and S5d). This underscores that a history of breast cancer did not significantly impact the observed ECM effect, supporting the primary influence of BMI or breast density on our proteomic results.

We also scored the available Hematoxylin and Eosin (H&E) scans of the samples to assess the level of adiposity, scar formation, fat necrosis, and immune infiltration (Supplementary Table 3). An insignificant level of immune infiltration and fat necrosis was observed in the samples, supporting the relatively normal state of the samples at the time of donation (Supplementary Table 3). Our analysis revealed an elevated percentage of adipose tissue correlated with increasing BMI (Fig. 5a, 5b, and 5d). The tissues used in this research effectively reflect the patient's BMI when considering the percentage of adiposity of the breast histology slides and tissue subsequently used for proteomics. Scar formation was reduced in obese individuals, inversely reflecting heightened BMI (Fig. 5c). Interestingly, there was no significant correlation, positive or negative, between percentage of adiposity and scar formation or percentage of adiposity and breast density (Fig. S4d and S4e). This reveals a significant decrease in breast density in obese individuals, reinforcing the independent roles of obesity and breast density as risk factors for breast cancer. Importantly, a patient's history of breast cancer did not

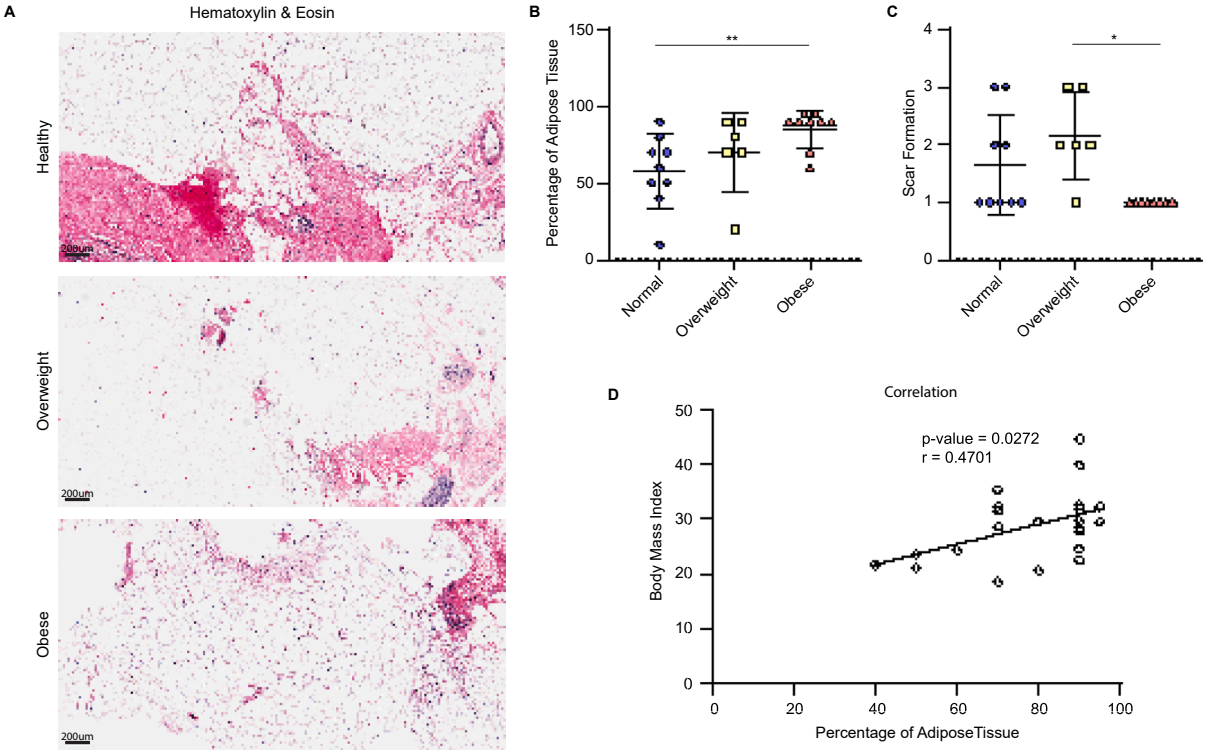

Fig. 5. Breast tissue adiposity is elevated in obese individuals. **(A)** 10x H&E images representative of the mean adiposity of normal weight, overweight, and obese patient breast samples. **(B)** Percentage of adipose tissue present in H&E slides of breast tissue from healthy, overweight, and obese patients. **(C)** Scar formation was scored on a scale of no scarring (1), focal scarring (2), and scarring (3). *Kruskal-Wallis Test* * $p \leq 0.05$, ** $p \leq 0.01$. **(D)** The correlation of body mass index to the percentage of adipose tissue. *Simple Linear Regression.*

significantly impact our observed effects, emphasizing the dominant influence of BMI.

Discussion

The ECM, which normally functions to maintain tissue homeostasis and provides a physical barrier between cells and tissues, is commonly dysregulated in both obesity and breast cancer [3,5,8,14]. Obesity induces a chronic inflammatory process characterized by adipose tissue hypertrophy and aberrant ECM remodeling, resulting in fibrosis and stromal stiffening [4,9]. Similarly, in the context of breast cancer, significant alterations to the organization, mechanics, and deposition of the ECM are present [5,11,43]. These changes can promote cancer progression, influencing growth, angiogenesis, and metastasis [5,11,34,43,44].

Using a novel two-fraction ECM extraction proteomic approach, we sought to clarify how obesity affects the ECM of normal breast tissue, identifying novel ECM-modifying proteins with implications on breast cancer outcomes [16]. We observed significant changes in the ECM of obese individuals, marked by elevated levels of structural basement membrane and vasculature-associated ECM proteins. Additionally, obese individuals showed an increased presence of ECM-modifying proteins regulating these tissue compartments. We consistently identified the protein PXDN throughout our analysis as a top-hit in obese individuals. The targets LGALS1 and LGALS3 were similarly identified as important ECM regulators in this patient cohort. These protein signatures appeared to be primarily attributable to fibroblasts, adipocytes, and to a lesser extent macrophages.

PXDN, a heme-containing peroxidase, plays a critical role in maintaining the basement membrane [19,20]. It functions through the preferential formation of hypobromous acid from hydrogen peroxide (H_2O_2) and bromide, which mediates the cross-linking of the C-terminal NC1 domain of collagen IV [19,20]. PXDN is currently the only known collagen IV crosslinker and is essential for the maintenance of basement membrane stiffness during development and in adult tissue [19]. Although heightened H_2O_2 levels in metabolic and fibrotic diseases promote PXDN levels and activity, a direct link to obesity has not been identified until now [45,46]. Our research establishes a clear link between PXDN and obesity in human breast tissue, emphasized by a robust correlation with pro-angiogenic ECM signatures. This connection is evident through the association of PXDN with other key proteins involved in vascular and basement membrane organization, including laminins, nidogens, and annexins. Previous studies have demonstrated that PXDN plays a pivotal role in vascular remodeling, influencing key processes like vasodilation, vascular tube formation, and vascular permeability [46–48]. Our findings connect these prior observations to measurable alterations in ECM composition potentially underlying these processes.

Elevated stromal stiffness is associated with solid tumor development, and in breast cancer, it further fuels aggressiveness, invasiveness, and metastasis [8]. Despite its crucial role in maintaining basement membrane stiffness, PXDN's involvement in cancer biology is just emerging, with studies investigating its effects on melanoma, ovarian, and prostate cancer [49,50]. In these cases, PXDN regulates cancer cell survival, invasion, migration, and metastasis [49,50]. While its influence on breast cancer proliferation has been noted in a *PIK3CA* mutated MCF10A basal mammary cell model, its effects on other syngeneic and patient-derived breast cancer cell lines are unexplored [51]. PXDN also acts as an effector in conditioned media from bone marrow-derived mesenchymal stromal cells, inducing migration in breast cancer cells [52]. Our findings align with this, underscoring the role of mesenchymal stromal cells, such as fibroblasts and adipocytes, in PXDN expression in obese samples—an overlooked aspect in current literature. PXDN poses a promising avenue for discovery, enabling a targeted approach for the exploration of basement membrane mechanics on breast cancer signaling.

LGALS1 and LGALS3, members of the beta-galactoside-binding lectin family, are pivotal in immune response, cell adhesion, migration, angiogenesis, and cancer [17,18,49]. These galectins interact with a diverse range of ligands, specifically binding to N-linked or O-linked glycosylation sites on glycoproteins [53,54]. Their versatile functionality extends to both extracellular and intracellular domains, interacting with surface receptors, signaling proteins, and ECM components [53,54]. Our results affirm the roles of LGALS1 and LGALS3 in shaping breast cancer outcomes. LGALS1 and LGALS3 have also been implicated in obesity and other metabolic and fibrotic diseases [22,23,53,55,56]. Despite accumulating evidence for the roles of these galectins in obesity, angiogenesis, and breast cancer, they remain uninterrogated in models of obese breast cancer. The ready availability of therapeutic tools to inhibit these proteins will facilitate future studies of these molecules [53,56].

The escalating global prevalence of obesity underscores the critical need to decipher the molecular signals that may contribute to its role in breast cancer [1,3,10]. While traditional treatments remain effective, the persistent issues of resistance and relapse underscore the need to identify therapeutics that can enhance current strategies. Based on our presented data, a comprehensive investigation into the functional roles of PXDN, LGALS1, and LGALS3 is warranted and will hopefully provide further therapeutic insights. This strategy complements ongoing initiatives targeting ECM-modifying proteins like LOX and PLOD2 [5,57]. These proteins regulate tissue stiffness and fibrosis, which prevent drug accessibility and promote an immunosuppressive microenvironment in breast cancer [5,57]. Current research has proposed these therapies as a method to sensitize TNBC to conventional therapies including chemotherapy [57]. Moreover, regarding BMI as a biomarker for personalized therapies offers a promising way to improve risk assessment for breast cancer. This research advances scientific understanding and addresses critical gaps by providing biomarkers, refining patient selection criteria, and rationalizing the study of targeted therapeutics for enhanced breast cancer management within the context of obesity.

Materials and methods

Protein extraction & digestion

Samples were processed and extracted as previously described (Barrett, A. S. *et al.* Hydroxylamine chemical digestion for insoluble extracellular matrix characterization. *J. Proteome Res.* **16**, 4177–4184 (2017).). Tissues were delipidated in ice-cold (−20 °C) acetone by incubating for 30 min at −20 °C. The tissue was pelleted, and the supernatant was removed, allowing the pellet to dry. This tissue pellet was then powderized using liquid nitrogen and a ceramic mortar and pestle then lyophilized. Weighed tissue (approximately 5 mg of each) was homogenized in freshly prepared high-salt buffer (50 mM Tris-HCl, 3 M NaCl, 25 mM EDTA, 0.25 % w/v CHAPS, pH 7.5) containing 1 × protease inhibitor (Halt Protease Inhibitor, Thermo Scientific) at a concentration of 10 mg/mL. Homogenization took place in a bead beater (Bullet Blender Storm 24, Next Advance, 1 mm glass beads) for 3 min at 4 °C. Samples were then spun for 20 min 18 000 g at 4 °C, and the supernatant was removed and stored as fraction 1. A fresh aliquot of high-salt buffer was added to the remaining pellet at 10 mg/mL of the starting weight, vortexed at 4 °C for 15 min, and spun for 15 min. The supernatant was removed and stored as fraction 2. This high-salt extraction was repeated once more to generate fraction 3, after which freshly prepared guanidine extraction buffer (6 M guanidinium chloride adjusted to pH 9.0 with NaOH) was added at 10 mg/mL and vortexed for 1 h at room temperature. The samples were then spun for 15 min, and the supernatant was removed and stored as fraction 4. Fractions 1, 2, and 3 were combined, and all fractions were stored at − 20 °C until further analysis. The remaining pellets of each tissue representing insoluble ECM proteins were treated with freshly prepared hydroxylamine buffer (1 M NH2OH–HCl, 4.5 M guanidine–HCl, 0.2 M K2CO3, pH

adjusted to 9.0 with NaOH) at 10 mg/mL of the starting tissue weight. The samples were briefly vortexed, then incubated at 45 °C with end-over-end rotation for 17 h. Following incubation, the samples were spun for 15 min at 18 000 g, and the supernatant was removed and stored as fraction 5 at − 20 °C until further proteolytic digestion with trypsin. Enzymatic digestion of proteins was performed according to the FASP protocol as previously described (Wiśniewski, J. R., Zougman, A., Nagaraj, N. & Mann, M. Universal sample preparation method for proteome analysis. *Nat. Methods* **6**, 359–362 (2009)). 200 uL of extract from each fraction was loaded separately onto 10 kD MWCO filters then washed, reduced, and alkylated then digested with trypsin at 37 °C for 14 h as outlined in the protocol. Peptides were eluted with two washes of 75 uL 0.1 % FA and then cleaned with Solid Phase Extraction (SPE).

LC-MS/MS data acquisition

Samples were analyzed as previously described (Barrett, A. S., Maller, O., Pickup, M. W., Weaver, V. M. & Hansen, K. C. Compartment resolved proteomics reveals a dynamic matrisome in a biomechanically driven model of pancreatic ductal adenocarcinoma. *J. Immunol. Regen. Med.* **1**, 67–75 (2018).) on a Q Exactive HF mass spectrometer (Thermo Fisher Scientific) coupled to an EASY-nanoLC 1000 system through a nanoelectrospray source. Dried-down samples were reconstituted in 32 uL 0.1 % FA of which 8 uL was injected for LC-MS/MS analysis. The analytical column (100 mm i.d. x 150 mm fused silica capillary packed in-house with 2.7 μm 80 Å Cortex C18 resin (Phenomenex; Torrance, CA).). The flow rate was adjusted to 400 nL/min, and peptides were separated over a 120-minute linear gradient of 4–28 % ACN with 0.1 % FA. DIA data acquisition was performed using the instrument supplied Xcalibur™ (version 2.1) software.

Data analysis

Raw data was initially analyzed using Scaffold DIA (Version 2.0.0) against SwissProt (20,405 sequences) restricted to Homo Sapiens using staggered windows. Precursor tolerance was set to ± 10 ppm and fragment tolerance was set to ± 15 ppm, allowing for 1 missed cleavage. Trypsin-specific cleavages at the C-terminal of K and R except after P were used for cell and sECM fractions, while HA/trypsin-specific cleavages were used for the iECM fraction. Carbamidomethyl (C) was used as a fixed modification for all fractions. Variable modifications were set as oxidation (M), Gln->pyro-Glu (N-term Q), deamidated (NQ), and acetyl (Protein N-term), with oxidation (P) (hydroxyproline) added for the two ECM fractions. Peptide and protein identifications were filtered to 1 % FDR. Quantification was performed using Encyclopedia (0.9.2). For each peptide, the 5 highest-quality fragment ions were selected for quantitation.

Data analysis by MetaboAnalyst

One-factor statistical analysis was employed to normalize and subsequently analyze the total protein peak intensities. Samples were categorized based on body mass index (BMI) into normal (18.5 to < 25 kg/m^2), overweight (25 to < 30 kg/m^2), and obese (≥ 30 kg/m^2) groups. The data were structured in columns for samples and rows for features, then analyzed in an unpaired manner. Normalization of samples was performed by sum and autoscaling, wherein each variable was mean-centered and divided by its standard deviation. The normalized protein peak intensities were exported for dot-plot generation and analysis using a Kruskal-Wallis test. The data editor was utilized to select two groups for comparison via a volcano plot. Additionally, a pattern search was conducted to determine the correlation of a feature of interest with other features or predefined profiles of normal-overweight-obese using Pearson R correlation tests. K-means clustering was performed on row-normalized protein peak intensity to generate heatmaps. Gene lists were generated for each cluster and processed for pathway analysis using Metascape.

Histopathology scoring

Aperio scans were retrieved from the Komen Tissue Bank for all samples except K105310 and K106505. These scans had resolutions of up to 20x and were obtained from Hematoxylin and Eosin (H&E) stained tissue slides. Each scan was evaluated by a licensed pathologist and tissue characteristics were scored. Scar formation and fat necrosis were classified into three categories: No (scored as 1, indicating absence), Focal (scored as 2, indicating localized presence), and Yes (scored as 3, indicating widespread presence). The percentage of adipose tissue represents the level of adipose tissue abundance with the slide scan. Type of immune infiltrate was categorized into lymphocytes, histiocytes, neutrophils, and plasma cells. The location of immune infiltrate was sorted into interlobular stroma, intralobular stroma, and adipose.

Mammogram scoring

Mammograms were obtained from the Komen Tissue Bank for all samples, except for K104628 and K106919, which lacked available mammograms and were thus excluded from analysis. Mammogram imaging was conducted to capture both mediolateral oblique and craniocaudal views, depending on the patient's risk. A licensed radiologist scored all available mammograms, typically spanning several years, according to the Breast Imaging Reporting & Data System (BI-RADS) criteria established by the American College of Radiology. This assessment evaluates breast density by comparing the proportion of glandular or connective tissue to adipose tissue in the mammogram. The BI-RADS scoring system categorizes breast density into four levels: A. Almost entirely fatty (scored as 1), B. Scattered areas of fibroglandular density (scored as 2), C. Heterogeneously dense (scored as 3), and D. Extremely dense (scored as 4).

Survival curves

Survival curves for relapse-free survival, overall survival, and distant metastasis-free survival were generated using the Kaplan-Meier Plotter. The following Affy IDs 212012_at, 201105_at, and 208949_s_at were used to generate survival curves for PXDN, LGALS1, and LGALS3 respectively. Patients were split by median and plots for basal and HER2 + samples were generated according to PAM50 subtyping. Statistical significance was calculated using the Log-rank test.

Funding

This work was funded by the National Cancer Institute (T32CA190216-06 to EB and R01CA205044 and R01CA258766 to PK) and the Cancer Center Support Grant (P30CA046934).

CRediT authorship contribution statement

Ellen E. Bamberg: Conceptualization, Data curation, Investigation, Writing – original draft, Formal analysis. **Mark Maslanka:** Investigation, Formal analysis. **Kiran Vinod-Paul:** Formal analysis. **Sharon Sams:** Formal analysis. **Erica Pollack:** Formal analysis. **Matthew Conklin:** Writing – review & editing, Project administration, Funding acquisition, Conceptualization. **Peter Kabos:** Writing – review & editing, Project administration, Funding acquisition, Conceptualization. **Kirk C. Hansen:** Writing – review & editing, Project administration, Methodology, Funding acquisition, Conceptualization.

Declaration of competing interest

The authors declare the following financial interests/personal relationships which may be considered as potential competing interests:

Peter Kabos reports financial support was provided by National Cancer Institute. Ellen Bamberg reports financial support was provided by National Cancer Institute. Kirk Hansen reports financial support was provided by University of Colorado Cancer Center. If there are other authors, they declare that they have no known competing financial interests or personal relationships that could have appeared to influence the work reported in this paper.

Data availability

This data has been deposited to the ProteomeXchange Consortium via the PRIDE partner repository (Project Accession: PXD051458; Project Name: Breast tissue and cancer proteomics).

Acknowledgments

Gratitude and admiration to Patricia Keely whose invaluable contributions not only made this study possible but also served as an inspiration throughout. Your expertise and dedication have left an indelible mark on our work, and we are forever grateful for your guidance and support.

Data from the Susan G. Komen Tissue Bank at the IU Simon Cancer Center was used in this study. We thank contributors, including Indiana University who collected data used in this study, as well as donors and their families, whose help and participation made this work possible.

Appendix A. Supplementary data

Supplementary data to this article can be found online at https://doi.org/10.1016/j.mbplus.2024.100162.

References

[1] M. Picon-Ruiz, C. Morata-Tarifa, J.J. Valle-Goffin, E.R. Friedman, J.M. Slingerland, Obesity and adverse breast cancer risk and outcome: Mechanistic insights and strategies for intervention, CA Cancer J. Clin. 67 (5) (2017) 378–397.

[2] F. Karatas, G.U. Erdem, S. Sahin, A. Aytekin, D. Yuce, A.R. Sever, T. Babacan, O. Ates, Y. Ozisik, K. Altundag, Obesity is an independent prognostic factor of decreased pathological complete response to neoadjuvant chemotherapy in breast cancer patients, Breast 32 (2017) 237–244.

[3] C. Koliaki, M. Dalamaga, S. Liatis, Update on the obesity epidemic: after the sudden rise, is the upward trajectory beginning to flatten? Curr. Obes. Rep. 12 (4) (2023) 514–527.

[4] E.A. Wellberg, P. Kabos, A.E. Gillen, B.M. Jacobsen, H.M. Brechbuhl, S.J. Johnson, M.C. Rudolph, S.M. Edgerton, A.D. Thor, S.M. Anderson, A. Elias, X.K. Zhou, N. M. Iyengar, M. Morrow, D.J. Falcone, O. El-Hely, A.J. Dannenberg, C.A. Sartorius, P.S. MacLean, FGFR1 underlies obesity-associated progression of estrogen receptor-positive breast cancer after estrogen deprivation, JCI Insight 3 (14) (2018).

[5] O. Maller, A.P. Drain, A.S. Barrett, S. Borgquist, B. Ruffell, I. Zakharevich, T. T. Pham, T. Gruosso, H. Kuasne, J.N. Lakins, I. Acerbi, J.M. Barnes, T. Nemkov, A. Chauhan, J. Gruenberg, A. Nasir, O. Bjarnadottir, Z. Werb, P. Kabos, Y.Y. Chen, E.S. Hwang, M. Park, L.M. Coussens, A.C. Nelson, K.C. Hansen, V.M. Weaver, Tumour-associated macrophages drive stromal cell-dependent collagen crosslinking and stiffening to promote breast cancer aggression, Nat. Mater. 20 (4) (2021) 548–559.

[6] H.J. Chen, X.Y. Yan, A. Sun, L. Zhang, J. Zhang, Y.E. Yan, Adipose extracellular matrix deposition is an indicator of obesity and metabolic disorders, J. Nutr. Biochem. 111 (2023) 109159.

[7] E.N. Devericks, M.S. Carson, L.E. McCullough, M.F. Coleman, S.D. Hursting, The obesity-breast cancer link: a multidisciplinary perspective, Cancer Metastasis Rev. 41 (3) (2022) 607–625.

[8] S. Sahin, G.U. Erdem, F. Karatas, A. Aytekin, A.R. Sever, Y. Ozisik, K. Altundag, The association between body mass index and immunohistochemical subtypes in breast cancer, Breast 32 (2017) 227–236.

[9] G. Marcelin, E.L. Gautier, K. Clément, Adipose tissue fibrosis in obesity: etiology and challenges, Annu. Rev. Physiol. 84 (2022) 135–155.

[10] H.-L. Nguyen, T. Geukens, M. Maetens, S. Aparicio, A. Bassez, A. Borg, J. Brock, A. Broeks, C. Caldas, F. Cardoso, M. De Schepper, M. Delorenzi, C.A. Drukker, A.M. Glas, A.R. Green, E. Isnaldi, J. Eyfjörð, H. Khout, S. Knappskog, S. Krishnamurthy, S.R. Lakhani, A. Langerod, J.W.M. Martens, A.E. McCart Reed, L. Murphy, S. Naulaerts, S. Nik-Zainal, I. Nevelsteen, P. Neven, M. Piccart, C. Poncet, K. Punie, C. Purdie, E.A. Rakha, A. Richardson, E. Rutgers, A. Vincent-Salomon, P.T. Simpson, M.K. Schmidt, C. Sotiriou, P.N. Span, K.T.B. Tan, A. Thompson, S. Tommasi, K. Van Baelen, M. Van de Vijver, S. Van Laere, L. van't Veer, G. Viale, A. Viari, H. Vos, A.T. Witteveen, H. Wildiers, G. Floris, A.D. Garg, A. Smeets, D. Lambrechts, E. Biganzoli, F. Richard, C. Desmedt, Obesity-associated changes in molecular biology of primary breast cancer, Nature Communications 14(1) (2023) 4418.

[11] H.M. Brechbuhl, A.S. Barrett, E. Kopin, J.C. Hagen, A.L. Han, A.E. Gillen, J. Finlay-Schultz, D.M. Cittelly, P. Owens, K.B. Horwitz, C.A. Sartorius, K. Hansen, P. Kabos, Fibroblast subtypes define a metastatic matrisome in breast cancer, JCI Insight 5 (4) (2020).

[12] C. Bodelon, M. Mullooly, R.M. Pfeiffer, S. Fan, M. Abubakar, P. Lenz, P.M. Vacek, D.L. Weaver, S.D. Herschorn, J.M. Johnson, B.L. Sprague, S. Hewitt, J. Shepherd, S. Malkov, P.J. Keely, K.W. Eliceiri, M.E. Sherman, M.W. Conklin, G.L. Gierach, Mammary collagen architecture and its association with mammographic density and lesion severity among women undergoing image-guided breast biopsy, Breast Cancer Res. 23 (1) (2021) 105.

[13] A.L. Wishart, S.J. Conner, J.R. Guarin, J.P. Fatherree, Y. Peng, R.A. McGinn, R. Crews, S.P. Naber, M. Hunter, A.S. Greenberg, M.J. Oudin, Decellularized extracellular matrix scaffolds identify full-length collagen VI as a driver of breast cancer cell invasion in obesity and metastasis, Sci. Adv. 6 (43) (2020).

[14] S.J. Conner, H.B. Borges, J.R. Guarin, T.J. Gerton, A. Yui, K.J. Salhany, D. N. Mensah, G.A. Hamilton, G.H. Le, K.C. Lew, C. Zhang, M.J. Oudin, Obesity Induces Temporally Regulated Alterations in the extracellular matrix that drive breast tumor invasion and metastasis, Cancer Res. (2024).

[15] V.M. Garrisi, A. Tufaro, P. Trerotoli, I. Bongarzone, M. Quaranta, V. Ventrella, S. Tommasi, G. Giannelli, A. Paradiso, Body mass index and serum proteomic profile in breast cancer and healthy women: a prospective study, PLoS One 7 (11) (2012) e49631.

[16] M.C. McCabe, L.R. Schmitt, R.C. Hill, M. Dzieciatkowska, M. Maslanka, W. F. Daamen, T.H. van Kuppevelt, D.J. Hof, K.C. Hansen, Evaluation and refinement of sample preparation methods for extracellular matrix proteome coverage, Mol. Cell. Proteomics 20 (2021) 100079.

[17] A.S. Barrett, M.J. Wither, R.C. Hill, M. Dzieciatkowska, A. D'Alessandro, J.A. Reisz, K.C. Hansen, Hydroxylamine chemical digestion for insoluble extracellular matrix characterization, J. Proteome Res. 16 (11) (2017) 4177–4184.

[18] S. Hudson, K. Vik Hjerkind, S. Vinnicombe, S. Allen, C. Trewin, G. Ursin, I. Dos-Santos-Silva, B.L. De Stavola, Adjusting for BMI in analyses of volumetric mammographic density and breast cancer risk, Breast Cancer Res 20(1) (2018) 156.

[19] K.E. Peebles, K.S. LaFever, P.S. Page-McCaw, S. Colon, D. Wang, A.M. Stricker, N. Ferrell, G. Bhave, A. Page-McCaw, Peroxidasin is required for full viability in development and for maintenance of tissue mechanics in adults, Matrix Biol. (2023).

[20] G. Bhave, C.F. Cummings, R.M. Vanacore, C. Kumagai-Cresse, I.A. Ero-Tolliver, M. Rafi, J.S. Kang, V. Pedchenko, L.I. Fessler, J.H. Fessler, B.G. Hudson, Peroxidasin forms sulfilimine chemical bonds using hypohalous acids in tissue genesis, Nat. Chem. Biol. 8 (9) (2012) 784–790.

[21] A.D. Theocharis, D. Manou, N.K. Karamanos, The extracellular matrix as a multitasking player in disease, FEBS J. 286 (15) (2019) 2830–2869.

[22] V.L. Thijssen, R. Postel, R.J. Brandwijk, R.P. Dings, I. Nesmelova, S. Satijn, N. Verhofstad, Y. Nakabeppu, L.G. Baum, J. Bakkers, K.H. Mayo, F. Poirier, A. W. Griffioen, Galectin-1 is essential in tumor angiogenesis and is a target for antiangiogenesis therapy, PNAS 103 (43) (2006) 15975–15980.

[23] M.Z.I. Pranjol, D.A. Zinovkin, A.R.T. Maskell, L.J. Stephens, S.L. Achinovich, D.M. Los', E.A. Nadyrov, M. Hannemann, N.J. Gutowski, J.L. Whatmore, Cathepsin L-induced galectin-1 may act as a proangiogenic factor in the metastasis of high-grade serous carcinoma, Journal of Translational Medicine 17(1) (2019) 216.

[24] R. Siddhartha, M. Garg, Interplay between extracellular matrix remodeling and angiogenesis in tumor ecosystem, Mol. Cancer Ther. 22 (3) (2023) 291–305.

[25] S.V. Ivanov, K.L. Rose, S. Colon, R.M. Vanacore, B.G. Hudson, G. Bhave, P. Voziyan, Identification of brominated proteins in renal extracellular matrix: potential interactions with peroxidasin, Biochem. Biophys. Res. Commun. 681 (2023) 152–156.

[26] V.L. Martins, M.P. Caley, K. Moore, Z. Szentpetery, S.T. Marsh, D.F. Murrell, M. H. Kim, M. Avari, J.A. McGrath, R. Cerio, A. Kivisaari, V.M. Kähäri, K. Hodivala-Dilke, C.H. Brennan, M. Chen, J.F. Marshall, E.A. O'Toole, Suppression of TGFβ and angiogenesis by type VII collagen in cutaneous SCC, J. Natl Cancer Inst. 108 (1) (2016).

[27] A.P. South, M. Laimer, M. Gueye, J.Y. Sui, L.F. Eichenfield, J.E. Mellerio, A. Nyström, Type VII collagen deficiency in the oncogenesis of cutaneous squamous cell carcinoma in dystrophic epidermolysis bullosa, J. Invest. Dermatol. 143 (11) (2023) 2108–2119.

[28] S. Christian, R. Winkler, I. Helfrich, A.M. Boos, E. Besemfelder, D. Schadendorf, H. G. Augustin, Endosialin (Tem1) is a marker of tumor-associated myofibroblasts and tumor vessel-associated mural cells, Am. J. Pathol. 172 (2) (2008) 486–494.

[29] C.-H. Pai, S.-R. Lin, C.-H. Liu, S.-Y. Pan, H. Hsu, Y.-T. Chen, C.-T. Yen, I.S. Yu, H.-L. Wu, S.-L. Lin, S.-W. Lin, Targeting fibroblast CD248 attenuates CCL17-expressing macrophages and tissue fibrosis, Sci. Rep. 10 (1) (2020) 16772.

[30] P. Petrus, T.L. Fernandez, M.M. Kwon, J.L. Huang, V. Lei, N.S. Safikhan, S. Karunakaran, D.J. O'Shannessy, X. Zheng, S.B. Catrina, E. Albone, J. Laine, K. Virtanen, S.M. Clee, T.J. Kieffer, C. Noll, A.C. Carpentier, J.D. Johnson, M. Rydén, E.M. Conway, Specific loss of adipocyte CD248 improves metabolic health via reduced white adipose tissue hypoxia, fibrosis and inflammation, EBioMedicine 44 (2019) 489–501.

[31] U. Lendahl, L. Muhl, C. Betsholtz, Identification, discrimination and heterogeneity of fibroblasts, Nat. Commun. 13 (1) (2022) 3409.

[32] J. Shin, S. Toyoda, Y. Okuno, R. Hayashi, S. Nishitani, T. Onodera, H. Sakamoto, S. Ito, S. Kobayashi, H. Nagao, S. Kita, M. Otsuki, A. Fukuhara, K. Nagata, I. Shimomura, HSP47 levels determine the degree of body adiposity, Nat. Commun. 14 (1) (2023) 7319.

[33] T. Miyamura, N. Sakamoto, K. Ishida, T. Kakugawa, H. Taniguchi, Y. Akiyama, D. Okuno, A. Hara, T. Kido, H. Ishimoto, T. Miyazaki, K. Matsumoto, T. Tsuchiya, H. Yamaguchi, T. Miyazaki, Y. Obase, Y. Ishimatsu, T. Nagayasu, H. Mukae, Presence of heat shock protein 47-positive fibroblasts in cancer stroma is associated with increased risk of postoperative recurrence in patients with lung cancer, Respir. Res. 21 (1) (2020) 234.
[34] M. Papanicolaou, A.L. Parker, M. Yam, E.C. Filipe, S.Z. Wu, J.L. Chitty, K. Wyllie, E. Tran, E. Mok, A. Nadalini, J.N. Skhinas, M.C. Lucas, D. Herrmann, M. Nobis, B. A. Pereira, A.M.K. Law, L. Castillo, K.J. Murphy, A. Zaratzian, J.F. Hastings, D. R. Croucher, E. Lim, B.G. Oliver, F.V. Mora, B.L. Parker, D. Gallego-Ortega, A. Swarbrick, S. O'Toole, P. Timpson, T.R. Cox, Temporal profiling of the breast tumour microenvironment reveals collagen XII as a driver of metastasis, Nat. Commun. 13 (1) (2022) 4587.
[35] M. Aikio, H. Elamaa, D. Vicente, V. Izzi, I. Kaur, L. Seppinen, H.E. Speedy, D. Kaminska, S. Kuusisto, R. Sormunen, R. Heljasvaara, E.L. Jones, M. Muilu, M. Jauhiainen, J. Pihlajamäki, M.J. Savolainen, C.C. Shoulders, T. Pihlajaniemi, Specific collagen XVIII isoforms promote adipose tissue accrual via mechanisms determining adipocyte number and affect fat deposition, PNAS 111 (30) (2014) E3043–E3052.
[36] C.S. Leung, T.-L. Yeung, K.-P. Yip, S. Pradeep, L. Balasubramanian, J. Liu, K.-K. Wong, L.S. Mangala, G.N. Armaiz-Pena, G. Lopez-Berestein, A.K. Sood, M. J. Birrer, S.C. Mok, Calcium-dependent FAK/CREB/TNNC1 signalling mediates the effect of stromal MFAP5 on ovarian cancer metastatic potential, Nat. Commun. 5 (1) (2014) 5092.
[37] S.W. Duffy, O.W.E. Morrish, P.C. Allgood, R. Black, M.G.C. Gillan, P. Willsher, J. Cooke, K.A. Duncan, M.J. Michell, H.M. Dobson, R. Maroni, Y.Y. Lim, H. N. Purushothaman, T. Suaris, S.M. Astley, K.C. Young, L. Tucker, F.J. Gilbert, Mammographic density and breast cancer risk in breast screening assessment cases and women with a family history of breast cancer, Eur. J. Cancer 88 (2018) 48–56.
[38] S. Byström, M. Eklund, M.-G. Hong, C. Fredolini, M. Eriksson, K. Czene, P. Hall, J. M. Schwenk, M. Gabrielson, Affinity proteomic profiling of plasma for proteins associated to area-based mammographic breast density, Breast Cancer Res. 20 (1) (2018) 14.
[39] J. Melnikow, J.J. Fenton, E.P. Whitlock, D.L. Miglioretti, M.S. Weyrich, J. H. Thompson, K. Shah, Supplemental screening for breast cancer in women with dense breasts: a systematic review for the U.S. preventive services task force, Ann. Intern. Med. 164 (4) (2016) 268–278.
[40] N.J. Engmann, C.G. Scott, M.R. Jensen, S. Winham, D.L. Miglioretti, L. Ma, K. Brandt, A. Mahmoudzadeh, D.H. Whaley, C. Hruska, F. Wu, A.D. Norman, R. A. Hiatt, J. Heine, J. Shepherd, V.S. Pankratz, C.M. Vachon, K. Kerlikowske, Combined effect of volumetric breast density and body mass index on breast cancer risk, Breast Cancer Res. Treat. 177 (1) (2019) 165–173.
[41] S.M. Advani, W. Zhu, J. Demb, B.L. Sprague, T. Onega, L.M. Henderson, D.S. M. Buist, D. Zhang, J.T. Schousboe, L.C. Walter, K. Kerlikowske, D.L. Miglioretti, D. Braithwaite, Association of breast density with breast cancer risk among women aged 65 years or older by age group and body mass index, JAMA Netw. Open 4 (8) (2021) e2122810.
[42] O. McGinn, D. Riley, J. Finlay-Schultz, K.V. Paul, P. Kabos, C.A. Sartorius, Cytokeratins 5 and 17 maintain an aggressive epithelial state in basal-like breast cancer, Mol. Cancer Res. 20 (9) (2022) 1443–1455.
[43] H.M. Brechbuhl, J. Finlay-Schultz, T.M. Yamamoto, A.E. Gillen, D.M. Cittelly, A. C. Tan, S.B. Sams, M.M. Pillai, A.D. Elias, W.A. Robinson, C.A. Sartorius, P. Kabos, Fibroblast subtypes regulate responsiveness of luminal breast cancer to estrogen, Clin. Cancer Res. 23 (7) (2017) 1710–1721.
[44] L.A. Tomko, R.C. Hill, A. Barrett, J.M. Szulczewski, M.W. Conklin, K.W. Eliceiri, P. J. Keely, K.C. Hansen, S.M. Ponik, Targeted matrisome analysis identifies thrombospondin-2 and tenascin-C in aligned collagen stroma from invasive breast carcinoma, Sci. Rep. 8 (1) (2018) 12941.
[45] M. Sojoodi, D.J. Erstad, S.C. Barrett, S. Salloum, S. Zhu, T. Qian, S. Colon, E. M. Gale, V.C. Jordan, Y. Wang, S. Li, B. Ataeinia, S. Jalilifiroozinezhad, M. Lanuti, L. Zukerberg, P. Caravan, Y. Hoshida, R.T. Chung, G. Bhave, G.M. Lauer, B. C. Fuchs, K.K. Tanabe, Peroxidasin deficiency re-programs macrophages toward pro-fibrolysis function and promotes collagen resolution in liver, Cell. Mol. Gastroenterol. Hepatol. 13 (5) (2022) 1483–1509.
[46] Y. An, B.-T. Xu, S.-R. Wan, X.-M. Ma, Y. Long, Y. Xu, Z.-Z. Jiang, The role of oxidative stress in diabetes mellitus-induced vascular endothelial dysfunction, Cardiovasc. Diabetol. 22 (1) (2023) 237.
[47] C. Jing, G. Zhang, Z. Liu, Q. Xu, C. Li, G. Cheng, R. Shi, Peroxidasin promotes diabetic vascular endothelial dysfunction induced by advanced glycation end products via NOX2/HOCl/Akt/eNOS pathway, Redox Biol. 45 (2021) 102031.
[48] V. Panagopoulos, I. Zinonos, D.A. Leach, S.J. Hay, V. Liapis, A. Zysk, W.V. Ingman, M.O. DeNichilo, A. Evdokiou, Uncovering a new role for peroxidase enzymes as drivers of angiogenesis, Int. J. Biochem. Cell Biol. 68 (2015) 128–138.
[49] K. Wyllie, V. Panagopoulos, T.R. Cox, The role of peroxidasin in solid cancer progression, Biochem. Soc. Trans. 51 (5) (2023) 1881–1895.
[50] M. Paumann-Page, N.F. Kienzl, J. Motwani, B. Bathish, L.N. Paton, N.J. Magon, B. Sevcnikar, P.G. Furtmüller, M.W. Traxlmayr, C. Obinger, M.R. Eccles, C. C. Winterbourn, Peroxidasin protein expression and enzymatic activity in metastatic melanoma cell lines are associated with invasive potential, Redox Biol. 46 (2021) 102090.
[51] C.D. Young, L.J. Zimmerman, D. Hoshino, L. Formisano, A.B. Hanker, M.L. Gatza, M.M. Morrison, P.D. Moore, C.A. Whitwell, B. Dave, T. Stricker, N.E. Bhola, G. O. Silva, P. Patel, D.M. Brantley-Sieders, M. Levin, M. Horiates, N.A. Palma, K. Wang, P.J. Stephens, C.M. Perou, A.M. Weaver, J.A. O'Shaughnessy, J.C. Chang, B.H. Park, D.C. Liebler, R.S. Cook, C.L. Arteaga, Activating PIK3CA mutations induce an epidermal growth factor receptor (EGFR)/extracellular signal-regulated kinase (ERK) paracrine signaling axis in basal-like breast cancer, Mol. Cell. Proteomics 14 (7) (2015) 1959–1976.
[52] F. Graf, P. Horn, A.D. Ho, M. Boutros, C. Maercker, The extracellular matrix proteins type I collagen, type III collagen, fibronectin, and laminin 421 stimulate migration of cancer cells, FASEB J. 35 (7) (2021) e21692.
[53] A. Bartolazzi, Galectins in cancer and translational medicine: from bench to bedside, Int. J. Mol. Sci. 19 (10) (2018).
[54] J.M. Cousin, M.J. Cloninger, The role of galectin-1 in cancer progression, and synthetic multivalent systems for the study of galectin-1, Int. J. Mol. Sci. 17 (9) (2016).
[55] J.H. Baek, D.H. Kim, J. Lee, S.J. Kim, K.H. Chun, Galectin-1 accelerates high-fat diet-induced obesity by activation of peroxisome proliferator-activated receptor gamma (PPARγ) in mice, Cell Death Dis. 12 (1) (2021) 66.
[56] M. Stasenko, E. Smith, O. Yeku, K.J. Park, I. Laster, K. Lee, S. Walderich, E. Spriggs, B. Rueda, B. Weigelt, D. Zamarin, T.D. Rao, D.R. Spriggs, Targeting galectin-3 with a high-affinity antibody for inhibition of high-grade serous ovarian cancer and other MUC16/CA-125-expressing malignancies, Sci. Rep. 11 (1) (2021) 3718.
[57] O. Saatci, A. Kaymak, U. Raza, P.G. Ersan, O. Akbulut, C.E. Banister, V. Sikirzhytski, U.M. Tokat, G. Aykut, S.A. Ansari, H.T. Dogan, M. Dogan, P. Jandaghi, A. Isik, F. Gundogdu, K. Kosemehmetoglu, O. Dizdar, S. Aksoy, A. Akyol, A. Uner, P.J. Buckhaults, Y. Riazalhosseini, O. Sahin, Targeting lysyl oxidase (LOX) overcomes chemotherapy resistance in triple negative breast cancer, Nat. Commun. 11 (1) (2020) 2416.